X-Ray Speckle Contrast Variation across Absorption Edges

Cornelia C. Retsch and Ian McNulty
Argonne National Laboratory, 9700 S. Cass Avenue, Argonne, Illinois 60439
(Received 3 October 2000; published 30 July 2001)

We measured static x-ray speckle contrast variation with the incident photon energy across a sample-specific absorption edge. In this paper, we present a theoretical description of this energy dependency consistent with our data. We found that the contrast depends mainly on the imaginary part of the complex index of refraction in the sample, as well as on the instrumental resolution. The speckle contrast decreases as the absorption cross section in the sample increases at the absorption edge. This result is not predicted by commonly used theory.

DOI: 10.1103/PhysRevLett.87.077401 PACS numbers: 78.70.Ck, 41.50.+h, 42.25.Kb, 42.30.Ms

Techniques involving the interaction of coherent light with condensed matter (speckle techniques) have been introduced to the x-ray regime during recent years (see, e.g., [1–8]). Most of these experiments, however, were done at photon energies above 5 keV. We are extending these techniques into the 1 to 4 keV range, an energy range that includes many important x-ray absorption edges, e.g., in Al, Si, P, S, the rare earths, and others. Recently, absorption edges in this energy region were used in magnetic speckle experiments [9,10]. To our knowledge, the effect of absorption edges on x-ray speckle contrast has not yet been studied. Standard speckle contrast theory does not predict any effect [11,12]. Still, contrast variation at sample-specific absorption edges can be of interest, for example, when samples composed of two or more elements are investigated. With a variation in contrast at a sample-specific absorption edge, one could enhance or suppress speckle originating from one or more of the constituent elements. In addition, edge-dependent contrast variations should be well understood if pre-, on-, and post-edge measurements are to be compared. In this Letter, we present edge-dependent x-ray speckle contrast measurements and a theoretical description of our observations.

Speckles are formed when a disordered system is illuminated with temporally and spatially coherent light. The wave fronts originating from the various scattering centers in the sample interfere, giving rise to speckle, a complex pattern of maxima and minima in the Fraunhofer limit of observation. The distribution, size, and contrast of the speckles give information about the sample, as well as the experimental setup, such as the degree of coherence. A useful tool for the statistical analysis of these speckle patterns is given by the normalized, baseline-subtracted intensity autocorrelation function $\Gamma_r(\Delta r)$ [11,12]:

$$\Gamma_r(\Delta r) = \frac{\langle I(r) I(r + \Delta r)\rangle_r}{\langle I(r)\rangle_r^2} - 1, \qquad (1)$$

where $\langle I(r)\rangle_r$ is the intensity in the speckle pattern at a position r on the detector, averaged over a region around r that is large compared to the size of one speckle. If the sample structure can be considered to be spatially uncorrelated, $\Gamma_r(\Delta r)$ is given by

$$\Gamma_r(\Delta r) = \alpha^2 \exp(-\Delta q_z^2 T^2 - \Delta q_r^2 D^2), \qquad (2)$$

where T is the thickness of the sample, D is the diameter of the illuminated area on it, and α is the degree of spatial coherence across this area. Δq_z and Δq_r are the differences in momentum transfer between two points of interest in the speckle pattern, split into components along and perpendicular to the beam, $\vec{q} = \vec{k}_{\text{in}} - \vec{k}_{\text{out}}$. The width of Γ_r is a measure for the average width of a speckle at position r on the detector; the height of Γ_r [i.e., $\Gamma_r(0)$] gives the contrast of the speckle pattern.

In the nonmonochromatic case, $\Gamma_r(\Delta q)$ has to be considered instead of $\Gamma_r(\Delta r)$. In order to write the explicit dependence of Γ_r on Δr, the autocorrelation function has now to be written as $\Gamma_r(k_1, k_2, \Delta r)$, where k_1 and k_2 are the magnitudes of two wave vectors. A two-dimensional convolution with the distribution of wave numbers k present in the experiment yields the autocorrelation function $\Gamma_{r,W}(\Delta r)$:

$$\Gamma_{r,W}(\Delta r) = \frac{\iint W(k_1) W(k_2) \Gamma_r(k_1, k_2, \Delta r) \langle I(k_1, r)\rangle_r \langle I(k_2, r)\rangle_r \, dk_1 \, dk_2}{[\int W(k) \langle I(k, r)\rangle_r \, dk]^2}, \qquad (3)$$

where $W(k)$ is the monochromator spectral response function and $\langle I(k, r)\rangle_r$ is the intensity in the speckle pattern at wave number k and position r, averaged over a region around r, as before. The overall level of contrast depends strongly on the width of $W(k)$ [12]. A sharp $W(k)$ (good monochromaticity) yields good contrast; a broad spectral response yields poor contrast. Usually it is assumed that $\langle I(k, r)\rangle_r$ does not vary significantly with k over the width of $W(k)$. Then Eq. (3) would simplify to

$$\tilde{\Gamma}_{r,W}(\Delta r) = \int W(k_1) W(k_2) \Gamma_r(k_1, k_2, \Delta r) \, dk_1 \, dk_2, \qquad (4)$$

which yields analytical results for a Gaussian profile $W(k)$ [12] and therefore would be convenient to use for the statistical analysis of speckle patterns. Near absorption edges, however, $\langle I(k,r)\rangle_r$ may vary significantly with k. Therefore, Eq. (3) has to be used without further simplification. Earlier treatments [11,12] neglect this case, and therefore are not applicable in the vicinity of absorption edges.

The experiments were performed at the SRI-CAT undulator beam line 2-ID-B [13,14] at the Advanced Photon Source. We investigated samples made of metallic zinc powder consisting of ~100 nm grains, which may agglomerate to 1 to 2 μm in size. The powder samples were supported on 200-nm-thick silicon nitride membranes.

Figure 1 shows a schematic of the experimental setup. The disordered powder samples were illuminated with a nearly coherent x-ray beam of 10 μm in diameter. The degree of coherence across this area was measured to be higher than 92% [15,16]. A germanium knife edge was used to block parasitic scattering to one side of the direct beam. We used a back-side-illuminated, liquid-nitrogen-cooled charge-coupled-device (CCD) camera to record the x-ray speckle patterns in direct-detection mode; the CCD was aligned in the shadow region of the knife edge. An avalanche photodiode detector (APD) was exchanged with the CCD to allow for transmission measurements. Speckle patterns were acquired as the incident photon energy was varied across the zinc $2p^{3/2}$ (L_{III}) absorption edge at 1021.8 eV. The measurements were done at three different energy resolution settings: 1.80, 3.48, and 6.25 eV, determined by various settings of the 2-ID-B spherical grating monochromator slits [14]. We analyzed the two-dimensional CCD images by calculating the normalized intensity autocorrelation functions at various locations in the patterns after normalizing to the integrated intensity as well as the q dependence of the intensity $S(q)$ in each pattern. This removed the effect of a decrease in intensity due to sample attenuation at the edge. This can be done because the speckle contrast, as defined above, is *independent* of the total intensity I_{tot} in the speckle patterns.

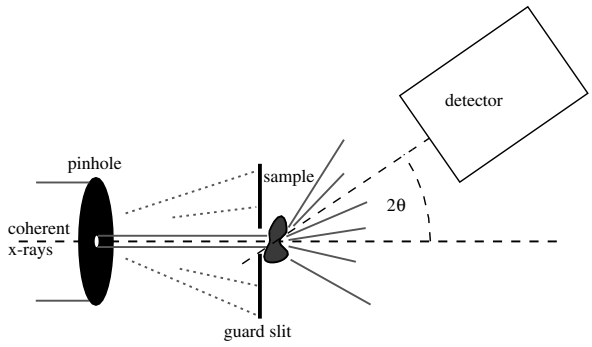

FIG. 1. The experimental setup. A pinhole of 10 μm diameter determined the beam size on the sample. Parasitic scattering was blocked by the guard slit. As a detector, we used a directly back-side-illuminated, liquid-nitrogen-cooled CCD camera.

Example speckle pictures as taken at 3.48 eV resolution are shown in Fig. 2. The images are plotted on a logarithmic scale with the maximum of the color table adjusted to the maximum in the pattern, so that the effect of reduced contrast above the absorption edge is visible and not hidden in the overall intensity effect present in these raw data images. Figure 3 shows the contrast in the speckle pictures evaluated as a function of energy. Presented is the average behavior of the contrast in reciprocal space, which we also expect to follow Eq. (3). All q dependence is reflected in the error bars shown in the figures and the errors given for the fit parameters.

Equation (3) was fit to the data, allowing for just three free parameters: T, the mean thickness of the sample, where $T \ll D$; E_0, an energy offset to allow for miscalibration of the monochromator energy scale; and ΔI, an

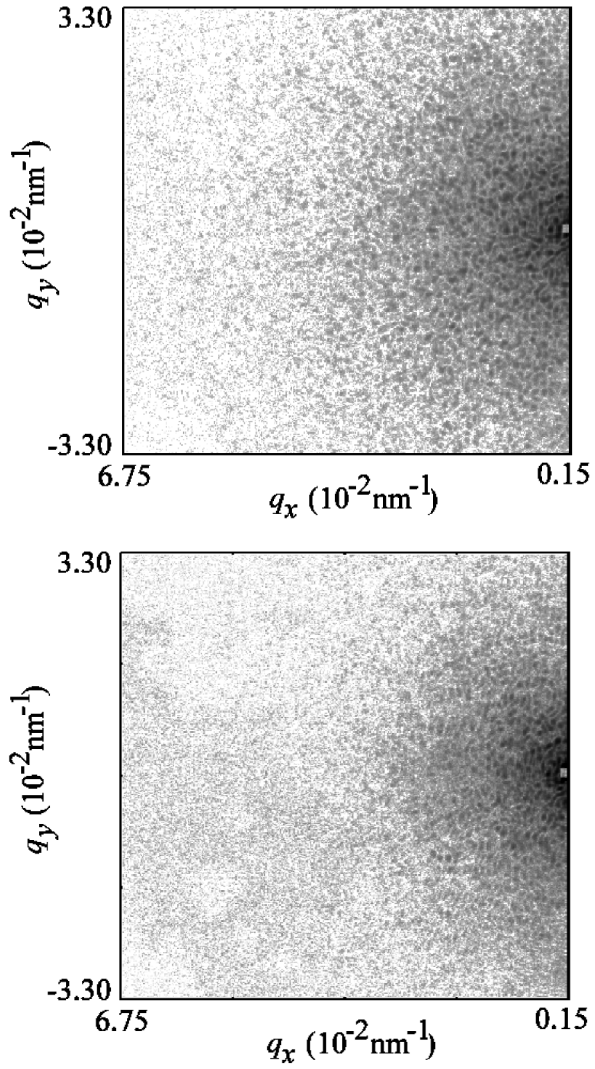

FIG. 2. Example speckle patterns from a zinc powder sample at 3.45 eV energy resolution as recorded with a CCD camera: below the L_{III} absorption edge at 1000 eV (top) and above the L_{III} absorption edge at 1030 eV (bottom).

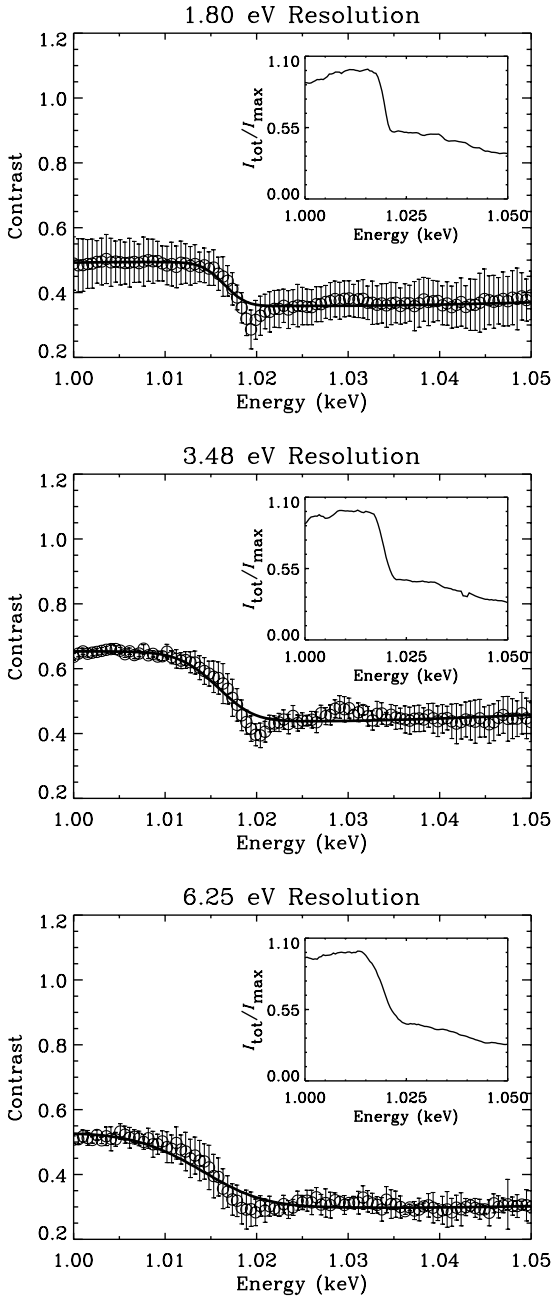

FIG. 3. X-ray speckle contrast versus energy in zinc powder samples at various energy resolutions: The symbols represent the contrast averaged over the region of interest in reciprocal space; all q dependence is reflected in the error bars. The solid lines show the fit of Eq. (3) to the data. The insets to the plots show the total transmitted intensity as measured with an APD directly behind the sample, normalized by the beam line efficiency.

intensity offset to allow for a small spectral background level. To account for the energy dependence of k in the sample, we assumed the usual expression $n = 1 - \delta - i\beta$ for the complex index of refraction. Thus, $\langle I(k,r)\rangle_r$ takes the simple form of $\exp(-2\beta kT)$ and $\Gamma_r(k_1,k_2,\Delta r)$ becomes $\Gamma_r[(1-\delta_1)k_1,(1-\delta_2)k_2,\Delta r]$. δ and β were taken from published values of the index of refraction [17,18]. For the spectral response function $W(k)$, we used a Gaussian around k_0 with standard deviation σ where 2.355σ is the energy resolution of the beam line [13], and accounted for E_0 and ΔI:

$$W(k) = \Delta I + \exp\left(\frac{-(k - k_0 - cE_0)^2}{2\sigma^2}\right), \qquad (5)$$

where c is the constant to convert energy into wave number. The fits are in good agreement with the data. Table I shows the resulting fit parameters and the q range covered in the measurements. From these, one can see that the energy calibration of the monochromator was offset by at least 4.7 eV. The background ΔI after monochromatization was less than 5% of the maximum intensity. This background level was probably due to parasitic scattering or higher-order spectral contamination from the monochromator. The variation in E_0 and ΔI with the slit settings is consistent with the known monochromator performance. On the other hand, the measurements at different energy resolutions were taken at different sample positions. Therefore, the fitted thicknesses differ slightly from one another. This effect is not related to the energy resolution. Still, the values are very similar, being $\approx$0.17 times the absorption length in Zn below the edge and $\approx$1.2 times above it. They agree well with the total transmission measurements (see insets of Fig. 3). More detailed structure in the contrast data may originate from structure in β, which is not found in the data of Henke and Hubbell [17,18], but could also be seen in the total transmission measurements. The dependence on the real part of the complex index of refraction cannot be seen in the contrast. This, as well as the dependence on β, can be understood by considering a Young's double-slit experiment with different thicknesses of sample in front of each slit. The different phase shifts across the two slits result only in a positional shift of the fringe pattern with no effect on the contrast. However, the differing intensities at the two slits result in decreased visibility [19]. The difference in intensities is smaller on the transmissive side of the edge than on the absorptive side. Thus, β influences the contrast. In all our measurements, we observe a decrease in speckle contrast at the edge.

We found a significant speckle contrast variation across the $2p^{3/2}$ absorption edge in powdered zinc samples, contrary to predictions [11,12]. Corresponding data we have taken across the K edge of a powdered aluminum sample yields comparable results. The speckle contrast *decreases* as the absorption cross section in the sample *increases* at the absorption edge. This implies the common assumption, that the energy dependence of the average intensity at a point in reciprocal space does not vary significantly over the width of the spectral response function, is no longer valid near an absorption edge. The simple model we used describes our data well and depends on a minimum of free parameters. This approach should be useful to characterize multicomponent samples by coherent x-ray techniques and

TABLE I. Fit parameters for the fit of Eq. (3) to the data for all three energy-resolution settings studied, as described in the text (see also Fig. 3). For each energy-resolution setting the q range covered is given.

Resolution eV	q 10^{-2} nm^{-1}	T μm	E_0 eV	$\Delta I/I_{\max}$ %
1.80	1.56 ± 0.43	0.10 ± 0.02	4.7 ± 0.6	1.7 ± 0.7
3.48	1.66 ± 0.49	0.16 ± 0.02	6.6 ± 0.7	1.4 ± 0.4
6.25	1.36 ± 0.32	0.22 ± 0.02	9.5 ± 1.3	4.8 ± 1.2

might be exploited for magnetic and other edge-dependent speckle measurements.

We thank Josef Arko, Sean P. Frigo, and Yuxin Wang for their support with the experimental setup and data collection, and Brian Tieman for the CCD camera acquisition program. We further thank G. Brian Stephenson for fruitful discussions. This work was supported by the U.S. Department of Energy, Basic Energy Science, Office of Science, under Contract No. W-31-109-Eng-38.

[1] M. Sutton, S. G. J. Mochrie, T. Greytak, S. E. Nagler, L. E. Berman, G. A. Held, and G. B. Stephenson, Nature (London) **352**, 608 (1991).

[2] Z. H. Cai, B. Lai, W. B. Yun, I. McNulty, K. G. Huang, and T. P. Russell, Phys. Rev. Lett. **73**, 82 (1994).

[3] A. Malik, A. R. Sandy, L. B. Lurio, G. B. Stephenson, S. G. J. Mochrie, I. McNulty, and M. Sutton, Phys. Rev. Lett. **81**, 5832 (1998).

[4] A. C. Price, L. B. Sorensen, S. D. Kevan, J. Toner, A. Poniewierski, and R. Holyst, Phys. Rev. Lett. **82**, 755 (1999).

[5] A. R. Sandy, L. B. Lurio, S. G. J. Mochrie, A. Malik, G. B. Stephenson, J. F. Pelletier, and M. Sutton, J. Synchrotron. Radiat. **6**, 1174 (1999).

[6] L. B. Lurio, D. Lumma, A. R. Sandy, M. A. Borthwick, P. Falus, S. G. J. Mochrie, J. F. Pelletier, M. Sutton, L. Regan, A. Malik, and G. B. Stephenson, Phys. Rev. Lett. **84**, 785 (2000).

[7] A. Fera, I. P. Dolbnya, G. Grübel, H. G. Muller, B. I. Ostrovskii, A. N. Shalaginov, and W. H. de Jeu, Phys. Rev. Lett. **85**, 2316 (2000).

[8] D. Lumma, L. B. Lurio, S. G. J. Mochrie, and M. Sutton, Rev. Sci. Instrum. **71**, 3274 (2000).

[9] F. Yakhou, A. Létoublon, F. Livet, M. de Boissieu, F. Bley, and C. Vettier, ESRF Newsletter **32**, 12 (1999).

[10] J. F. Peters, M. A. D. Vries, J. Miguel, O. Toulemonde, and J. B. Goedkoop, ESRF Newsletter **34**, 15 (2000); see also H. A. Dürr *et al.,* Science **284**, 2166 (1999).

[11] G. Parry, in *Laser Speckle and Related Phenomena,* edited by J. C. Dainty (Springer-Verlag, New York, 1984), Chap. 3.

[12] D. L. Abernathy, G. Grübel, S. Brauer, I. McNulty, G. B. Stephenson, S. G. J. Mochrie, A. R. Sandy, N. Mulders, and M. Sutton, J. Synchrotron. Radiat. **5**, 37 (1998).

[13] I. McNulty, A. M. Khounsary, Y. P. Feng, Y. Qian, J. Barraza, C. Benson, and D. Shu, Rev. Sci. Instrum. **67** (1996), CD-ROM.

[14] I. McNulty, Y. P. Feng, S. P. Frigo, and T. M. Mooney, in *Gratings and Grating Monochromators for Synchrotron Radiation,* edited by W. R. McKinney and C. A. Palmer (SPIE, San Diego, California, 1997), Vol. 3150, pp. 195–204.

[15] M. Born and E. Wolf, *Principles of Optics* (Cambridge University, Cambridge, England, 1997), 6th ed.

[16] D. Paterson, B. E. Allman, P. J. McMahon, J. Lin, N. Moldovan, K. A. Nugent, I. McNulty, C. T. Chantler, C. C. Retsch, T. H. K. Irving, and D. C. Mancini, Opt. Commun. (to be published).

[17] B. L. Henke, E. M. Gullikson, and J. C. Davis, At. Data Nucl. Data Tables **54**, 181 (1993).

[18] J. H. Hubbell, W. J. Veigele, E. A. Briggs, R. T. Brown, D. T. Cromer, and R. Howerton, J. Phys. Chem. Ref. Data **4**, 471 (1975); **6**, 615(E) (1977).

[19] J. Goodman, *Statistical Optics* (Wiley, New York, 1985).